IEEE Access
Multidisciplinary | Rapid Review | Open Access Journal

Received January 31, 2022, accepted February 22, 2022, date of publication March 2, 2022, date of current version March 10, 2022.

Digital Object Identifier 10.1109/ACCESS.2022.3156081

Security Constrained Unit Commitment Based on Modified Line Outage Distribution Factors

HUANSHENG ZHOU, (Member, IEEE), KANGLONG YUAN, AND CHENG LEI
Energy Development Research Institute, China Southern Power Grid, Guangzhou 510530, China

Corresponding author: Huansheng Zhou (ephuansheng@mail.scut.edu.cn)

This work was supported by the Energy Development Research Institute under Project EDRI-GH-KJXM-2020-101 and Project EDRI-GH-ZLKT-2020-201.

ABSTRACT The N-1 criterion is universally taken as the security constrains in the security-constrained unit commitment (SCUC) problem. The line outage distribution factors (LODF) is widely used in the N-1 continency for its state independence and computational efficiency. However, the LODF based model fails to consider reactive power and voltage magnitude. This paper closes this gap by deriving modified line outage distribution factors (MLODF) based on a linear power flow model. The proposed model, though state-independent, provides high-quality approximation of voltage magnitudes. Then, we apply this model to formulate the SCUC problem and propose an iterative solution process based on MLODF post-contingency filter to set up the contingency constraints. The simulation results of the benchmark test systems verify the accuracy of proposed MLODF. The six-bus and IEEE 118-bus systems show that the MLODF based model can provide a more accurate and secure generation schedule comparing with the traditional LODF based model while ensuring the AC feasibility for most N-1 continency.

INDEX TERMS Modified line outage distribution factor, state-independent, linear power flow model, mixed-integer linear programming, security constrained unit commitment.

I. INTRODUCTION

Security-constrained unit commitment (SCUC) refers to the economic dispatching of generating units for supplying the system load and satisfying the transmission network security at the normal state [1], which has been widely applied in both vertically integrated utilities and restructured power systems. The efficient solution framework for this problem is to implement iterative procedure between a master problem (unit commitment) and subproblems (network security evaluation). Reference [2] summarized some mainstream methodologies for solving the SCUC master problem and sub-problems in terms of modeling ability, feasibility and optimality, solution stability, computer resource consumption, post-contingency actions and CPU time.

Prevalent SCUC problems are based on the DC power flow formulation owe to its reasonable accuracy and computational efficiency [3], [4]. Reactive power constraints and bus voltage limits are not considered. However, during the actual operation of power system, a significant voltage drops across long-distance transmission is more likely to occur, which may cause the bus voltage to exceed its limit, especially at load center buses [5]. Besides, the reactive power flow may have a great influence on line current, particularly in power networks with strong coupling between active and reactive power [6], which may yield uneconomic or insecure solutions. Based on the two reasons above, SCUC problem considering AC power flow constraints is a necessity to improve grid operations. Reference [7] established a SCUC problem with AC constraint and applied the Benders decomposition for separating the unit commitment in the master problem from the network security check in subproblems. The authors of [8] proposed a solution technique based on the outer approximation method to co-optimize real and reactive power scheduling and dispatch subject to both unit commitment constraints and ACOPF constraints. In [9], a novel decomposition method is also proposed for the AC-SCUC problem. By solving the MISOCP model of the master problem, the active power and reactive power are co-optimized based on the conic approximations of the AC power flow equations.

However, the solution cannot guarantee the global optimum because of the non-convexity [10], [11]. To bridge this

The associate editor coordinating the review of this manuscript and approving it for publication was Behnam Mohammadi-Ivatloo.

gap, several linear power flow models considering the reactive power and voltage profiles are proposed. Reference [12] proposed the decoupled linearized power flow (DLPF) model with respect to voltage magnitude and phase angle. The model is state independent and the accuracy and robustness are proved in several cases, including radial distribution systems, meshed large-scale transmission systems and ill-conditioned systems. The authors of [13] derived a general linearized power flow model considering tap changers and phase shifters using the logarithmic transform of voltage magnitudes (LTVM). An improved linearized network model based on the Taylor series expansion was derived in [14]. The piece-wise linearization technique method with integer variables is applied to handle the nonconvexity introduced by the quadratic losses. A linearized power flow model that preserves the effect of reactive power was developed in [15]. Reference [16] proposed an approximate power flow solution for a distribution network, in which the voltage phasor was approximated as a linear function of load demands at PQ buses with guaranteed error bounds. Reference [17] employed curve fitting to linearize the nonlinear terms of voltages in the power flow model. These models provide high-quality approximation of AC power model while maintaining the computation efficiency, having been applied to the optimal power flows [18], [19], transmission expansion planning [20].

In the contingency security assessment, the line outages are often considered because of their universality. The most classical method is to use the line outage distribution factors (LODF) [21, [22], which can be directly calculated according to the power transfer distribution factors (PTDF) of the pre-contingency network [23]. PTDF de-scribes how the real power flows change if power injection is shifted from one node to another. Correspondingly, LODF describes how the flows change when one line fails. Awe to its computational efficiency, LODF has been widely used in generation capacity expansion planning problem [24], optimal power flow calculation [25], real-time operation [26] and SCUC problem [3]. Though LODF can straightly determine the post-contingency active power flow, it cannot predict post-outage reactive power flows and voltage. To solve this problem, many researchers also proposed the methods based on the sensitivity coefficients to calculate the post-contingency states [27], [28]. However, they are related to the system base points, which is difficult to apply in the SCUC problem.

The major contributions claimed in this paper are as follows:

- This paper proposes the modified line outage distribution factors (MLODF), which is derived from a state-independent linear power flow model and only related to the network parameters. The proposed factors are distinguished by their high-quality approximation of post-contingency active power flows and voltage magnitudes.
- A formulation for SCUC problems based on MLODF for post-contingency states is established and a linearization method is applied to approximate the quadratic branch flow limits.
- To improve the computational efficiency, an iterative solution process based on MLODF post-contingency filter is proposed to set up the contingency constraints.
- The simulation results on several different scales of power system verify the accuracy of the proposed MLODF model. The SCUC problem based on MLODF can provide a more secure generation schedule than the traditional LODF based model.

The remainder of this paper is organized as follows. Section II describes the derivation of MLODF. Section III introduces the formulation for the SCUC. Section IV presents the solution method based on the MLODF post-contingency filter. Section V contains the case study to verify the proposed model. Finally, Section VI draws the conclusions and suggestions in the future work.

II. DERIVATION OF MLODF

The line outage model through the incremental injections of buses is simulated in [29]. Figure 1 illustrates the simulation when the line nm is off. The incremental injecting power $(\Delta P_n + j\Delta Q_n,\ \ \Delta P_m + j\Delta Q_m)$ at the end bus n and bus m can be expressed by the flowing in the line nm in the final simulated state $(\tilde{P}_{nm} + j\tilde{Q}_{nm},\ \ \tilde{P}_{mn} + j\tilde{Q}_{mn})$ as follow:

$$\begin{aligned}\Delta P_n + j\Delta Q_n &= \left(P_n^* + jQ_n^*\right) - \left(\tilde{P}_n + j\tilde{Q}_n\right) = \tilde{P}_{nm} + j\tilde{Q}_{nm}\\ \Delta P_m + j\Delta Q_m &= \left(P_m^* + jQ_m^*\right) - \left(\tilde{P}_m + j\tilde{Q}_m\right) = \tilde{P}_{mn} + j\tilde{Q}_{mn}\end{aligned} \tag{1}$$

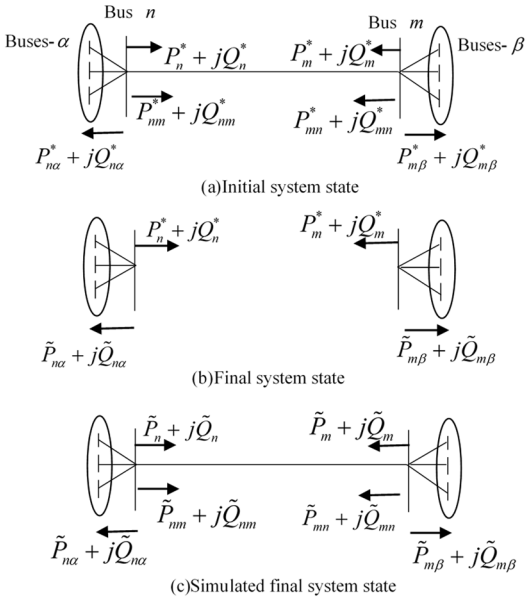

FIGURE 1. Line outage modeling using injections.

To make the AC power flow model non-convex, the following linear approximations [12] can be applied to decouple the voltage magnitudes and the phase angles in the power flow equations:

$$P_i = \sum_{j=1}^{n} g_{ij} V_j - \sum_{j=1}^{n} b'_{ij} \theta_j, \tag{2}$$

$$Q_i = -\sum_{j=1}^{n} b_{ij} V_j - \sum_{j=1}^{n} g_{ij} \theta_j. \tag{3}$$

where P_i and $Q_i$denote the net power injection of active and reactive power at bus i, respectively; $g_{ij}$and b_{ij} denote the real and imaginary part of nodal admittance; V_j and $\theta_j$denote the voltage magnitude and phase angle of bus j.

Based on (2) and (3), we can obtain the linear expression for branch flow as follow:

$$P_{ij} = g_{ij}(V_i - V_j) - b_{ij}(\theta_i - \theta_j) + g_{ij}^{\mathrm{sh}} V_i, \tag{4}$$

$$Q_{ij} = -b_{ij}(V_i - V_j) - g_{ij}(\theta_i - \theta_j) - b_{ij}^{\mathrm{sh}} V_i. \tag{5}$$

where $y_{ij}^{\mathrm{sh}} = g_{ij}^{\mathrm{sh}} + j b_{ij}^{\mathrm{sh}}$ are the line shunt admittance including the line-charging susceptance and equivalent admittance of transformers and phase shifters. According to [12], for branches with transformers and phase shifters, $y_{ij}^{\mathrm{sh}} = \frac{y_{ij}}{t^2} - \frac{y_{ij}}{t} e^{-j\theta_s}$, $y_{ji}^{\mathrm{sh}} = y_{ij} - \frac{y_{ij}}{t} e^{j\theta_s}$.

We can calculate perturbations for a given operating state by the first-order Taylor expansion of (4) and (5):

$$\begin{bmatrix} \Delta P \\ \Delta Q \end{bmatrix} = \begin{bmatrix} G & -B' \\ -B & -G \end{bmatrix} \begin{bmatrix} \Delta V \\ \Delta \theta \end{bmatrix}. \tag{6}$$

Then, the changes in voltage magnitude and the phase angle (ΔV, $\Delta\theta$), for given changes in the bus power injections (ΔP, ΔQ) can be written as:

$$\begin{bmatrix} \Delta V \\ \Delta \theta \end{bmatrix} = \begin{bmatrix} G & -B' \\ -B & -G \end{bmatrix}^{-1} \begin{bmatrix} \Delta P \\ \Delta Q \end{bmatrix} = \begin{bmatrix} H & N \\ K & L \end{bmatrix} \begin{bmatrix} \Delta P \\ \Delta Q \end{bmatrix}, \tag{7}$$

where

$$\Delta P = \begin{bmatrix} \vdots \\ \Delta P_n \\ \vdots \\ \Delta P_m \end{bmatrix}, \quad \Delta Q = \begin{bmatrix} \vdots \\ \Delta Q_n \\ \vdots \\ \Delta Q_m \end{bmatrix}. \tag{8}$$

So that

$$\begin{bmatrix} \Delta V_n \\ \Delta V_m \\ \Delta \theta_n \\ \Delta \theta_m \end{bmatrix} = \begin{bmatrix} H_{nn} & N_{nn} & H_{nm} & N_{nm} \\ H_{mn} & N_{mn} & H_{mm} & N_{mm} \\ K_{nn} & L_{nn} & K_{nm} & L_{nm} \\ K_{mn} & L_{mn} & K_{mm} & L_{mm} \end{bmatrix} \begin{bmatrix} \Delta P_n \\ \Delta Q_n \\ \Delta P_m \\ \Delta Q_m \end{bmatrix}. \tag{9}$$

Collating (4), (5) and (9), we can establish the relationship among the post-outage flowing in the line nm, the incremental injections into buses n, $m$and the pre-outage flowing in the line $nm(P_{nm}^*, Q_{nm}^*, P_{mn}^*, Q_{mn}^*)$ as follow:

$$\begin{bmatrix} \tilde{P}_{nm} \\ \tilde{Q}_{nm} \\ \tilde{P}_{mn} \\ \tilde{Q}_{mn} \end{bmatrix} = \begin{bmatrix} P_{nm}^* \\ Q_{nm}^* \\ P_{mn}^* \\ Q_{mn}^* \end{bmatrix} + \begin{bmatrix} HK_{11} & NL_{12} & HK_{13} & NL_{14} \\ HK_{21} & NL_{22} & HK_{23} & NL_{24} \\ HK_{31} & NL_{32} & HK_{33} & NL_{34} \\ HK_{41} & NL_{42} & HK_{43} & NL_{44} \end{bmatrix} \times \begin{bmatrix} \Delta P_n \\ \Delta Q_n \\ \Delta P_m \\ \Delta Q_m \end{bmatrix}. \tag{10}$$

Substituting (1) into (10) yields:

$$\begin{aligned} \begin{bmatrix} \tilde{P}_{nm} \\ \tilde{Q}_{nm} \\ \tilde{P}_{mn} \\ \tilde{Q}_{mn} \end{bmatrix} &= \begin{bmatrix} \Delta P_n \\ \Delta Q_n \\ \Delta P_m \\ \Delta Q_m \end{bmatrix} \\ &= \left(E - \begin{bmatrix} HK_{11} & NL_{12} & HK_{13} & NL_{14} \\ HK_{21} & NL_{22} & HK_{23} & NL_{24} \\ HK_{31} & NL_{32} & HK_{33} & NL_{34} \\ HK_{41} & NL_{42} & HK_{43} & NL_{44} \end{bmatrix} \right)^{-1} \\ &\quad \times \begin{bmatrix} P_{nm}^* \\ Q_{nm}^* \\ P_{mn}^* \\ Q_{mn}^* \end{bmatrix}. \end{aligned} \tag{11}$$

Through (7) and (11), we can get the increment of bus voltage:

$$\begin{aligned} \begin{bmatrix} \Delta V_i \\ \Delta \theta_i \end{bmatrix} &= \begin{bmatrix} H_{in} & N_{in} & H_{im} & N_{im} \\ K_{in} & L_{in} & K_{im} & L_{im} \end{bmatrix} \begin{bmatrix} \Delta P_n \\ \Delta Q_n \\ \Delta P_m \\ \Delta Q_m \end{bmatrix} \\ &= \begin{bmatrix} H'_{11} & N'_{12} & H'_{13} & N'_{14} \\ K'_{21} & L'_{22} & K'_{23} & L'_{24} \end{bmatrix} \begin{bmatrix} P_{nm}^* \\ Q_{nm}^* \\ P_{mn}^* \\ Q_{mn}^* \end{bmatrix}. \end{aligned} \tag{12}$$

We define several factors ($\alpha_{i,nm}, \beta_{i,nm}, \varepsilon_{i,nm}, \gamma_{i,nm}$) as the sensitivity coefficients of pre-outage power flows in the line nm to the incremental voltage at bus i. Therefore, the post-outage voltage can be written as:

$$\begin{aligned} \tilde{V}_i &= V_i^* + \Delta V_i \\ &= V_i^* + \alpha_{i,nm} P_{nm}^* + \beta_{i,nm} Q_{nm}^* + \alpha_{i,mn} P_{mn}^* + \beta_{i,mn} Q_{mn}^*, \end{aligned} \tag{13}$$

$$\begin{aligned} \tilde{\theta}_i &= \theta_i^* + \Delta\theta_i \\ &= \theta_i^* + \gamma_{i,nm} P_{nm}^* + \varepsilon_{i,nm} Q_{nm}^* + \gamma_{i,mn} P_{mn}^* + \varepsilon_{i,mn} Q_{mn}^*. \end{aligned} \tag{14}$$

While the power flowing over the line $ij$is equal to

$$\begin{cases} \tilde{P}_{ij} = P_{ij}^* + \Delta P_{ij} \\ \tilde{Q}_{ij} = Q_{ij}^* + \Delta Q_{ij} \\ \tilde{P}_{ji} = P_{ji}^* + \Delta P_{ji} \\ \tilde{Q}_{ji} = Q_{ji}^* + \Delta Q_{ji}, \end{cases} \tag{15}$$

where

$$\begin{aligned}\Delta P_{ij} &= g_{ij}\left(\Delta V_i - \Delta V_j\right) - b_{ij}\left(\Delta\theta_i - \Delta\theta_j\right) + g_{ij}^{\mathrm{sh}}\Delta V_i \\ &= \left[g_{ij}\left(\alpha_{i,nm} - \alpha_{j,nm}\right) - b_{ij}\left(\gamma_{i,nm} - \gamma_{j,nm}\right) + g_{ij}^{\mathrm{sh}}\alpha_{i,nm}\right]P_{nm}^{*} \\ &\quad + \left[g_{ij}\left(\beta_{i,nm} - \beta_{j,nm}\right) - b_{ij}\left(\varepsilon_{i,nm} - \varepsilon_{j,nm}\right) + g_{ij}^{\mathrm{sh}}\beta_{i,nm}\right]Q_{nm}^{*} \\ &\quad + \left[g_{ij}\left(\alpha_{i,mn} - \alpha_{j,mn}\right) - b_{ij}\left(\gamma_{i,mn} - \gamma_{j,mn}\right)\right]P_{mn}^{*} \\ &\quad + \left[g_{ij}\left(\beta_{i,mn} - \beta_{j,mn}\right) - b_{ij}\left(\varepsilon_{i,mn} - \varepsilon_{j,mn}\right)\right]Q_{mn}^{*} \\ &= LPP_{ij}^{nm}P_{nm}^{*} + LPQ_{ij}^{nm}Q_{nm}^{*} + LPP_{ij}^{mn}P_{mn}^{*} + LPQ_{ij}^{mn}Q_{mn}^{*}.\end{aligned} \tag{16}$$

Similar to (16), ΔP_{ji}, ΔQ_{ij}, ΔQ_{ji} can be expressed by the pre-outage flowing in line nm.

The coefficients of LPP_{ij}^{nm}, LPQ_{ij}^{nm}, LPP_{ij}^{mn}, LPQ_{ij}^{mn} in (16) are the MLODFs we proposed, e.g. LPP_{ij}^{hm} represents the change in active power transfer on line ij (ΔP_{ij}), with respect to the pre-outage active power flow on line nm (P_{nm}^{*}), as a result of the outage of line nm.

III. FORMULATION OF SCUC BASED ON MLODF

This section provides the detailed formulation of the objective function and constraints relevant to the SCUC model.

A. OBJECTIVE FUNCTION

The total production cost of all units is to be minimized. The operation cost of a thermal unit is defined as a linear function of variables:

$$\sum_{t\in\mathcal{T}}\sum_{g\in\mathcal{I}^{\mathrm{TU}}}\left(f_g^{\mathrm{TU}}(p_{g,t}) + c_g^{\mathrm{SU}}x_{g,t} + c_g^{\mathrm{SD}}y_{g,t} + c_g^{\mathrm{NL}}u_{g,t}\right), \tag{17}$$

where $\mathcal{T}, \mathcal{I}^{\mathrm{TU}}$ are the index for periods and thermal units; $f_g^{\mathrm{TU}}(\cdot)$ is the piecewise linear cost of the thermal unit; $c_g^{\mathrm{SU}}, c_g^{\mathrm{SD}}, c_g^{\mathrm{NL}}$ are the startup, shutdown and no-load cost of the unit, respectively; $x_{g,t}, y_{g,t}, u_{g,t}$ are the startup, shutdown and commitment decisions of the unit, respectively; $p_{g,t}$ is the active power output above the minimum output.

B. CONSTRAINTS

1) ELECTRIC POWER BALANCE CONSTRAINTS

$$\begin{aligned}&\sum_{j\in\mathcal{I}^{\mathrm{bus}}}G_{ij}V_{j,t} - \sum_{j\in\mathcal{I}^{\mathrm{bus}}}B'_{ij}\theta_{j,t} \\ &\quad = \sum_{g\in\mathcal{S}_i^{\mathrm{TU}}}(pg,t + ug,t\underline{P}g) - PDi,t,\end{aligned} \tag{18}$$

$$\begin{aligned}&-\sum_{j\in\mathcal{I}^{\mathrm{bus}}}B_{ij}V_{j,t} - \sum_{j\in\mathcal{I}^{\mathrm{bus}}}G_{ij}\theta_{j,t} \\ &\quad = \sum_{g\in\mathcal{S}_i^{\mathrm{TU}}}(qg,t + ug,t\underline{Q}g) - QDi,t,\end{aligned} \tag{19}$$

where $\mathcal{I}^{\mathrm{bus}}$ are the index for buses in the electricity network; $\mathcal{S}_i^{\mathrm{TU}}$ are the index of thermal units connecting to the bus i; $\underline{P}_g$, $\underline{Q}g$ are the minimum generation active and reactive output; $PD_{i,t}$, $QD_{i,t}$ are the active and reactive demand; $q_{g,t}$ is the reactive power output above the minimum output.

2) Spinning reserve constraints:

$$\begin{aligned}p_{g,t} + ru_{g,t} \le (\bar{P}_g - P_g)u_{g,t} - (\bar{P}_g - SU_g)x_{g,t}, \\ MU_g = 1,\end{aligned} \tag{20}$$

$$\begin{aligned}p_{g,t} + ru_{g,t} \le (\bar{P}_g - P_g)u_{g,t} - (\bar{P}_g - SD_g)y_{g,t+1}, \\ MU_g = 1,\end{aligned} \tag{21}$$

$$\begin{aligned}p_{g,t} + ru_{g,t} \le (\bar{P}_g - P_g)u_{g,t} - (\bar{P}_g - SU_g)x_{g,t} \\ - (\bar{P}_g - SD_g)y_{g,t+1}, \quad MU_g \ge 2\end{aligned} \tag{22}$$

$$rd_{g,t} - p_{g,t} \le 0, \tag{23}$$

$$\sum_{g\in\mathcal{I}^{\mathrm{TU}}}ru_{g,t} \ge SR^{\mathrm{up}}, \quad \sum_{g\in\mathcal{I}^{\mathrm{TU}}}rd_{g,t} \ge SR^{\mathrm{down}}, \tag{24}$$

where MU_g is the minimum uptime of the unit; $\bar{P}_g$ is the maximum generation active output; SU_g, SD_g are the startup and shutdown ramping capability of the unit; $SR^{\mathrm{up}}, SR^{\mathrm{down}}$ are system-wide upward and downward spinning reserve capacity requirement; $ru_{g,t}$, $rd_{g,t}$ are upward and downward spinning reserve of the unit.

3) Ramping constraints:

$$-RD_g \le p_{g,t} - p_{g,t-1} \le RU_g, \tag{25}$$

where RU_g, RD_g are upward and downward ramping capability of the unit.

4) Logic constraints of unit commitment states:

$$u_{g,t} - u_{g,t-1} = x_{g,t} - g_{g,t}, \tag{26}$$

$$\sum_{\tau=\max\{1,t-MU_g+1\}}^{t}x_{g,\tau} \le u_{g,t}, \tag{27}$$

$$\sum_{\tau=\max\{1,t-MD_g+1\}}^{t}y_{g,\tau} \le 1 - u_{g,t}, \tag{28}$$

$$u_{g,t} \in \{0,1\},\ 0 \le x_{g,t} \le 1,\ 0 \le y_{g,t} \le 1, \tag{29}$$

where $MD_{g,t}$ is the minimum downtime of the unit.

5) Reactive generation limit constraints:

$$q_{g,t} + u_{g,t}\underline{Q}_g \le u_{g,t}\bar{Q}_g, \tag{30}$$

where $\bar{Q}_g$ is the maximum generation reactive output.

6) Pre-Outage network constraints:

$$\begin{aligned}P_{ij,t} &= g_{ij}(V_{i,t} - V_{j,t}) - b_{ij}(\theta_{i,t} - \theta_{j,t}) + g_{ij}^{\mathrm{sh}}V_{i,t} \\ Q_{ij,t} &= -b_{ij}(V_{i,t} - V_{j,t}) - g_{ij}(\theta_{i,t} - \theta_{j,t}) - b_{ij}^{\mathrm{sh}}V_{i,t},\end{aligned} \tag{31}$$

$$\begin{aligned}&P_{ij,t}^2 + Q_{ij,t}^2 \le (\bar{S}_{ij})^2 \\ &P_{ji,t}^2 + Q_{ji,t}^2 \le (\bar{S}_{ij})^2 \\ &\quad \underline{V}_i \le V_{i,t} \le \bar{V}_i,\end{aligned} \tag{32}$$

where $\overline{S}_{ij}$is the apparent power capacity of the transmission lines; $\underline{V}_i$, $\overline{V}_i$ are the minimum and maximum voltage magnitude of buses.

7) Post-Outage network constraints:

$$\begin{aligned}\tilde{P}_{ij}^{nm} &= P_{ij}^{*} + LPP_{ij}^{nm}P_{nm}^{*} + LPQ_{ij}^{nm}Q_{nm}^{*} + LPP_{ij}^{mn}P_{mn}^{*} \\ &\quad + LPQ_{ij}^{mn}Q_{mn}^{*} \\ \tilde{Q}_{ij}^{nm} &= Q_{ij}^{*} + LQP_{ij}^{nm}P_{nm}^{*} + LQQ_{ij}^{nm}Q_{nm}^{*} + LQP_{ij}^{mn}P_{mn}^{*} \\ &\quad + LQQ_{ij}^{mn}Q_{mn}^{*} \\ \tilde{V}_{i}^{nm} &= V_{i}^{*} + \alpha_{i,nm}P_{nm}^{*} + \beta_{i,nm}Q_{nm}^{*} + \alpha_{i,mn}P_{mn}^{*} \\ &\quad + \beta_{i,mn}Q_{mn}^{*}, \end{aligned} \tag{33}$$

$$\left(\tilde{P}_{ij,t}^{nm}\right)^2 + \left(\tilde{Q}_{ij,t}^{nm}\right)^2 \le \left(\overline{S'}_{ij}\right)^2$$

$$\left(\tilde{P}_{ji,t}^{nm}\right)^2 + \left(\tilde{Q}_{ji,t}^{nm}\right)^2 \le \left(\overline{S'}_{ij}\right)^2$$

$$\underline{V}_i' \le \tilde{V}_{i,t}^{nm} \le \bar{V}_i', \tag{34}$$

where $\overline{S'}_{ij}$ is the emergency apparent power capacity of the transmission lines; $\underline{V}_i'$, $\bar{V}_i'$ are the emergency voltage magnitude limit of buses.

IV. SOLUTION METHOD

A. FLOWCHART OF THE SCUC PROBLEM

Most of the N-1 contingency constraints are inactive and can be discarded [30]. To reduce the number of N-1 contingency constraints, we propose an iterative filtering process based on the MLODF to set up the contingency constraints. The flowchart of the MLODF post-contingency filter for the SCUC problem is shown in Figure 2.

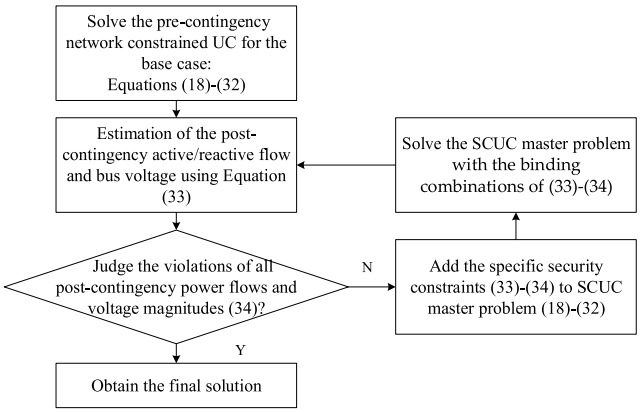

FIGURE 2. Flowchart of the MLODF post-contingency filter for the SCUC problem.

The solution procedure starts by calculating the pre-contingency network constrained UC, in which (18)-(32) will be included. The network constrained UC obtains the pre-contingency line flows (P_{ij}/Q_{ij}) and bus voltage (V_i). Then, the post-contingency filter uses (33) to compute all the post-contingency line ij power flows ($\tilde{P}_{ij,t}^{nm}$, $\tilde{Q}_{ij,t}^{nm}$) and bus voltage ($\tilde{V}_{i,t}^{nm}$) when the line nm fails according to (33). If all post-contingency power flows and voltage magnitudes are within their limiting values ($\Delta \le \overline{\Delta}$), the final solution is obtained. If the above condition is not satisfied, then the corresponding constraints in (33)-(34) are added to the SCUC master problem (18)-(32). After solving the SCUC with the binding combinations of (33)-(34), the pre-contingency flows and bus voltage are updated and analyzed again. This iterative approach provides an efficient way to find out the active contingencies to include in the SCUC.

B. LINEAR APPROXIMATION OF THE QUADRATIC CONSTRAINTS

Note that the transmission capacity constraints (32) and (34) are both quadratic items, which makes the scheduling problem nonlinear. To improve the computational efficiency, a linearization method is applied to approximate the quadratic branch flow limits [31]. The feasible region defined by these constraints can be represented by the area enclosed by a circle, which can be approximated by its inscribed n-side polygon, as shown in Figure 3.

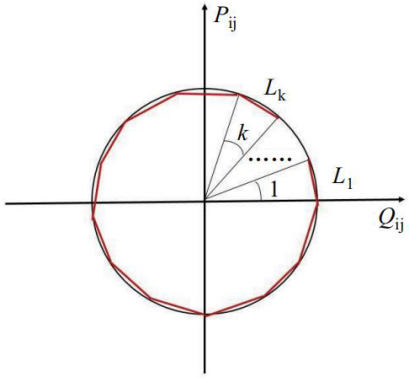

FIGURE 3. Linearization of the quadratic branch flow limits.

For a circle of radius r, each secant is related to an arc of $2\pi r/n$ length. The area inside the circle, typically defined by $x^2 + y^2 \le r^2$, can be approximated by n linear represented by:

$$\begin{aligned}\cot\frac{(2k-1)\pi}{n}x + y - r\sin\frac{2k\pi}{n} - r\cot\frac{(2k-1)\pi}{n} \\ \times \cos\frac{2k\pi}{n} \le 0, \quad \forall k = 1, 2, \ldots, n\end{aligned} \tag{35}$$

Then, the transmission capacity constraints (32) and (34) can be approximatively replaced with a series of linear constraints as follows:

$$\alpha_{ij}P_{ij} + \beta_{ij}Q_{ij} + \gamma_{ij} \ge 0, \quad \forall (i,j) \tag{36}$$

where α_{ij},β_{ij}, γ_{ij}correspond to the coefficients of x, y and the constant term in Equation (36), respectively.

V. CASE STUDY

Case studies are conducted to demonstrate the performance of the proposed MLODF model. In the first test, several benchmark power systems are applied to analyze the active power flows and voltage magnitudes under N-1 contingencies

to verify the accuracy of the proposed MLODF model. In the second experiment, the six-bus system and the IEEE 118-bus system are used to analyze the security performance of the proposed model. All the optimization problems are solved with the commercial solver Gurobi 8.1.1 using MATLAB R2016a.

A. ACCURACY VERIFICATION

A total of 5 benchmark power systems are employed as test examples, the sizes of which range from 6 to 2,383 buses with different loading conditions. All of the test data can be accessed online in the package of MATPOWER without any modification [32].

The following two models are compared: (1) the proposed MLODF, (2) the traditional LODF. Two important results, i.e., branch MW flows and voltage magnitudes are obtained for comparison. With the results of the AC power flow model (ACPF) as the benchmark, the root-mean-square errors of branch MW flows and voltage magnitudes are calculated, as shown in Figure 4 and Figure 5.

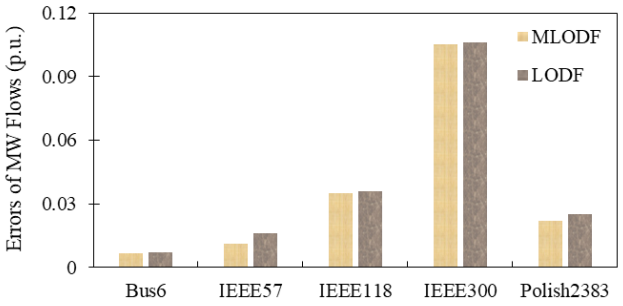

FIGURE 4. Root-mean-square errors of MW flows.

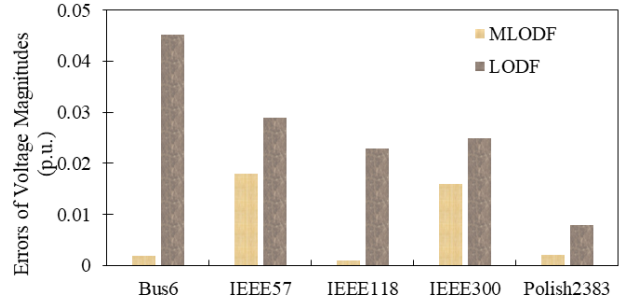

FIGURE 5. Root-mean-square errors of voltage magnitudes.

Obviously, MLODF model performs better than LODF model not only in active power flows but also in voltage magnitudes. Especially for the voltage magnitudes, the root-mean-square errors of MLODF are far smaller than those of LODF. This is because the proposed MLODF considers the influence of voltage and reactive power on the basis of LODF, resulting in a better approximate effect on ACPF. The simulation result also verifies the correctness of the MLODF derivation process.

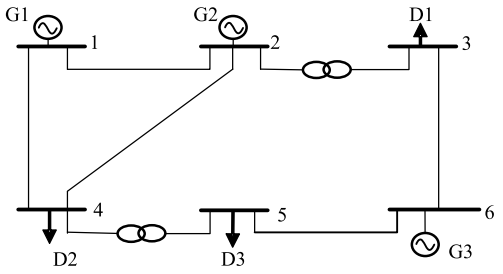

FIGURE 6. Diagram of the six-bus system.

B. SECURITY VERIFICATION

To illustrate the security of day-ahead scheduling solution obtained by the proposed MLODF model, we carry out a test in a six-bus electric power system. The six-bus system includes 3 generators and 7 transmission lines.

Table 1 shows the commitment schedules of SCUC based on MLODF model and LODF model, respectively. G3 is not committed at hours 9-24 when using traditional LODF based model due to the following reasons: (1) the traditional LODF based model fails to consider reactive power balance constraints. For hours 9-24, the total reactive load cannot be supplied by G1 alone. (2) the traditional LODF based model ignores the voltage constraints. For hours 9-24, if G1 is the only committed unit, the voltage of bus 2 will drop below its lower limit when the line 1-2 is tripped off. For this reason, the MLODF based model starts up G3 to improve the voltage of bus 2 in this condition. Therefore, the proposed MLODF based model considers the constraints of voltage and reactive power, which can provide a more secure generation schedule.

TABLE 1. Unit commitments obtained by two different models.

Model	Unit	1	2	3	4	5	6	7	8	9	10	11	12	13	14	15	16	17	18	19	20	21	22	23	24
MLODF	G1	0	0	0	0	0	0	1	1	1	1	1	1	1	1	1	1	1	1	1	1	1	1	1	1
	G2	1	1	1	1	1	1	1	1	0	0	0	0	0	0	0	0	0	0	0	0	0	0	0	0
	G3	0	0	0	0	0	0	0	0	1	1	1	1	1	1	1	1	1	1	1	1	1	1	1	1
LODF	G1	0	0	0	0	0	0	1	1	1	1	1	1	1	1	1	1	1	1	1	1	1	1	1	1
	G2	1	1	1	1	1	1	1	1	0	0	0	0	0	0	0	0	0	0	0	0	0	0	0	0
	G3	0	0	0	0	0	0	0	0	0	0	0	0	0	0	0	0	0	0	0	0	0	0	0	0

To further demonstrate the accuracy and security of the proposed MLODF model in the large-scale power systems, the IEEE 118-bus system is applied here. The IEEE 118-bus system includes 52 generators as well as 186 transmission lines. Figure 7 shows the commitment schedules of SCUC based on MLODF model and LODF model, respectively.

As shown in Figure 7, four more units are committed when using the proposed MLODF based model compared with the traditional LODF based model. They are G16 (connected to bus 36), G21 (connected to bus 54), G46 (connected to bus 103) and G50 (connected to bus 110), respectively. The MLODF based model starts up G16 to avoid the voltage of bus 39, 40 and 41 dropping below their lower limit under N-1 contingency, for its relatively lower operational cost than the

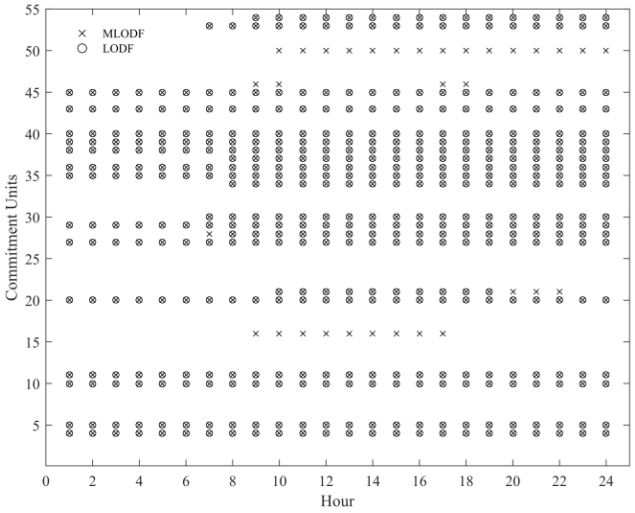

FIGURE 7. Unit commitments of IEEE 118-bus system.

other near units. Similarly, G46 and G50 are committed to improve the overall voltage of a local area, especially the bus 109, 110, 111 and 112 when the line 103-110 is tripped off. Additionally, to supply the reactive load of bus 54 at hours 10-22, G21 needs to run for a few more hours.

To investigate the AC feasibility of proposed model, we study the violation (where post-contingency power flows or voltage magnitudes are beyond their emergency limits) of AC power flow equations with the solutions. There still exist 108 voltage violations and 48 line flowing violations, which account for 1.36% in the whole set of N-1 contingency. Those voltage violations mainly from bus 39, 40 and 41 when the line 37-39 fails, as well as from bus 109, 110, 111 and 112 when the line 103-110 fails. Those line flowing violations mainly from line 47-69 and line 49-69 when line 65-68 fails. But for the other more than 98% contingencies, the line flowing and bus voltage are secure within their limits.

To analyze the influence of serious contingency to accuracy, Figures 8-10 visualize the solutions for the worst situation in terms of the maximum voltage magnitude and MW flow errors at hour 17. As shown in Figure 8, the voltage magnitudes of bus 39, 40 and 41 drop below their lower limit. This is because when line 37-39 fails, the reactive

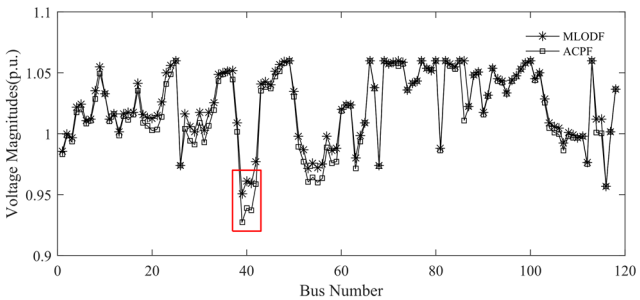

FIGURE 8. Voltage magnitudes at hour 17 when the line 37-39 is off.

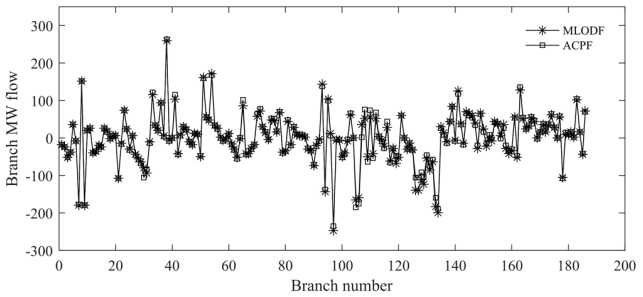

FIGURE 9. Branch MW flow at hour 17 when the line 65-68 is off.

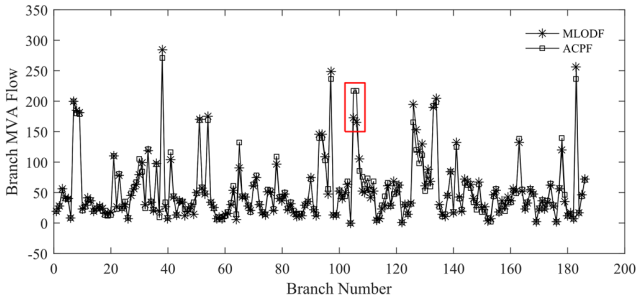

FIGURE 10. Branch MVA flow at hour 17 when the line 65-68 is off.

load of bus 39, 40 and 41 can't be supplied by the near unit directly. The voltage magnitudes of these buses drop to some extent, which deviates from the assumption on the state-independent linear power flow in [12], thus resulting in a great error. From Figure 9, we can see that the MLODF based model is still accurate in approximating MW flows even in a scenario with a maximum error. Note that the complex flows of line 47-69 (branch number 105) and line 49-69 (branch number 106) are beyond their emergency limits when line 65-68 fails, as shown in Figure 10. This is because line 47-69 and line 49-69 both have a high reactance, which results in a large reactive power loss. However, the linearized power flow model used in this paper neglects the branch losses. Therefore, at this time, the MLODF based model has poor approximation effect on the reactive power of these two transmission lines, which produces larger errors to branch complex flows.

In summary, for few N-1 contingencies, if the bus voltage deviates from the rated value or the reactive power loss of the transmission line increases, the post-contingency voltage magnitudes or power flows may beyond their emergency limits. Under these N-1 contingency scenarios, the actual network power flow deviates from two basic assumptions. One is that all bus voltages of the state-independent linearized power flow model are assumed near to their rated values. The other is that the branch losses are neglected.

The total operational cost of the MLODF based model is 797,683.7$ while the traditional LODF based model is 794,533.0$. Though the MLODF based model incurs higher cost, it addresses the potential risks of voltage violation and

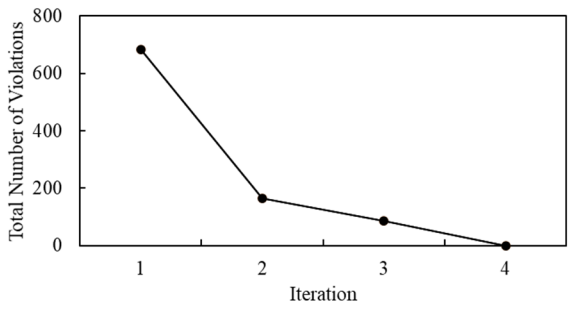

FIGURE 11. Iteration convergence.

complex flow violation for most N-1 contingency and thus provides a more secure generation schedule.

Figure 11 denotes the convergence performance of the proposed solution method. The solution time is 643.3s. The number of iterations in IEEE 118-bus system is 4 with a relative rap of 0.5%. The total number of limit violations of post-contingency power flows and voltage magnitudes is counted in each iteration. It is clear that the number of violations declines rapidly and the convergence performance of the solution method is acceptable.

Therefore, case studies above verify the accuracy and security of the proposed MLODF model and the effectiveness of the solution method based on MLODF post-contingency filter.

VI. CONCLUSION

In this paper, we propose the MLODF derived from a state-independent linear power flow model and apply this model to formulate the SCUC problem. The simulation results show that:

1) The proposed MLODF model can calculate post-outage voltage and active power flow through pre-outage line flowing and has a better approximate effect on ACPF than DCPF model. It holds the accuracy as the original state-independent linear power flow model, which also verifies the correctness of the MLODF derivation process.

2) The SCUC problem based on MLODF considers the constraints of voltage and reactive power, which provides a more secure generation schedule than the traditional LODF based model.

3) For most N-1 continencies, the generation schedule obtained by the MLODF based model can make sure that the line flowing and bus voltage are secure within their limits.

REFERENCES

[1] Y. Fu, M. Shahidehpour, and Z. Li, "AC contingency dispatch based on security-constrained unit commitment," *IEEE Trans. Power Syst.*, vol. 21, no. 2, pp. 897–908, May 2006.

[2] Y. Fu, Z. Li, and L. Wu, "Modeling and solution of the large-scale security-constrained unit commitment," *IEEE Trans. Power Syst.*, vol. 28, no. 4, pp. 3524–3533, Nov. 2013.

[3] D. A. Tejada-Arango, P. Sánchez-Martın, and A. Ramos, "Security constrained unit commitment using line outage distribution factors," *IEEE Trans. Power Syst.*, vol. 33, no. 1, pp. 329–337, Jan. 2018.

[4] H. Ye and Z. Li, "Robust security-constrained unit commitment and dispatch with recourse cost requirement," *IEEE Trans. Power Syst.*, vol. 31, no. 5, pp. 3527–3536, Sep. 2016.

[5] B. Stott, J. Jardim, and O. Alsac, "DC power flow revisited," *IEEE Trans. Power Syst.*, vol. 24, no. 3, pp. 1290–1300, Aug. 2009.

[6] K. Purchala, L. Meeus, D. Van Dommelen, and R. Belmans, "Usefulness of DC power flow for active power flow analysis," in *Proc. IEEE Power Eng. Soc. Gen. Meeting*, Jun. 2005, pp. 454–459.

[7] Y. Fu, M. Shahidehpour, and Z. Li, "Security-constrained unit commitment with AC constraints," *IEEE Trans. Power Syst.*, vol. 20, no. 2, pp. 1538–1550, Aug. 2005.

[8] A. Castillo, C. Laird, C. A. Silva-Monroy, J.-P. Watson, and R. P. O'Neill, "The unit commitment problem with AC optimal power flow constraints," *IEEE Trans. Power Syst.*, vol. 31, no. 6, pp. 4853–4866, Nov. 2016.

[9] Y. Bai, H. Zhong, Q. Xia, C. Kang, and L. Xie, "A decomposition method for network-constrained unit commitment with AC power flow constraints," *Energy*, vol. 88, pp. 595–603, Aug. 2015.

[10] Z. Yang, K. Xie, J. Yu, H. Zhong, N. Zhang, and Q. X. Xia, "A general formulation of linear power flow models: Basic theory and error analysis," *IEEE Trans. Power Syst.*, vol. 34, no. 2, pp. 1315–1324, Mar. 2019.

[11] Z. Yang, H. Zhong, Q. Xia, and C. Kang, "A novel network model for optimal power flow with reactive power and network losses," *Electr. Power Syst. Res.*, vol. 144, pp. 63–71, Mar. 2017.

[12] J. Yang, N. Zhang, C. Kang, and Q. Xia, "A state-independent linear power flow model with accurate estimation of voltage magnitude," *IEEE Trans. Power Syst.*, vol. 32, no. 5, pp. 3607–3617, Sep. 2017.

[13] Z. Li, J. Yu, and Q. H. Wu, "Approximate linear power flow using logarithmic transform of voltage magnitudes with reactive power and transmission loss consideration," *IEEE Trans. Power Syst.*, vol. 33, no. 4, pp. 4593–4603, Jul. 2018.

[14] H. Zhang, V. Vittal, G. T. Heydt, and J. Quintero, "A mixed-integer linear programming approach for multi-stage security-constrained transmission expansion planning," *IEEE Trans. Power Syst.*, vol. 27, no. 2, pp. 1125–1133, May 2012.

[15] S. M. Fatemi, S. Abedi, G. B. Gharehpetian, S. H. Hosseinian, and M. Abedi, "Introducing a novel DC power flow method with reactive power considerations," *IEEE Trans. Power Syst.*, vol. 30, no. 6, pp. 3012–3023, Nov. 2015.

[16] S. Bolognani and S. Zampieri, "On the existence and linear approximation of the power flow solution in power distribution networks," *IEEE Trans. Power Syst.*, vol. 31, no. 1, pp. 163–172, Jan. 2016.

[17] H. Ahmadi, J. R. Marti, and A. von Meier, "A linear power flow formulation three-phase distribution systems," *IEEE Trans. Power Syst.*, vol. 31, no. 6, pp. 5012–5021, Nov. 2016.

[18] Z. Yang, H. Zhong, Q. Xia, and C. Kang, "Solving OPF using linear approximations: Fundamental analysis and numerical demonstration," *IET Gener., Transmiss. Distrib.*, vol. 11, no. 17, pp. 4115–4125, Nov. 2017.

[19] Z. Yang, H. Zhong, and A. Bose, "A linearized OPF model with reactive power and voltage magnitude: A pathway to improve the MW-only DC OPF," *IEEE Trans. Power Syst.*, vol. 33, no. 2, pp. 1734–1745, Mar. 2018.

[20] H. Zhang, G. T. Heydt, and V. Vittal, "An improved network model for transmission expansion planning considering reactive power and network losses," *IEEE Trans. Power Syst.*, vol. 28, no. 3, pp. 3471–3479, Aug. 2013.

[21] T. Guler, G. Gross, and M. Liu, "Generalized line outage distribution factors," *IEEE Trans. Power Syst.*, vol. 22, no. 2, pp. 879–881, May 2007.

[22] J. Guo, Y. Fu, Z. Li, and M. Shahidehpour, "Direct calculation of line outage distribution factors," *IEEE Trans. Power Syst.*, vol. 24, no. 3, pp. 1633–1634, Aug. 2009.

[23] F. M. Gonzalez-Longatt and J. L. Rueda, *PowerFactory Applications for Power System Analysis*. Springer, 2014.

[24] V. H. Hinojosa and J. Velásquez, "Improving the mathematical formulation of security-constrained generation capacity expansion planning using power transmission distribution factors and line outage distribution factors," *Electr. Power Syst. Res.*, vol. 140, pp. 391–400, Nov. 2016.

[25] R. Spangler and R. Shoults, "Power generation, operation, and control," *IEEE Power Energy Mag.*, vol. 12, no. 4, pp. 90–93, Aug. 2014.

[26] J. Zhu, *Optimization of Power System Operation*. Tallinn, Estonia: Estonian Academy, 2009.

[27] P. A. Ruiz and P. W. Sauer, "Voltage and reactive power estimation for contingency analysis using sensitivities," *IEEE Trans. Power Syst.*, vol. 22, no. 2, pp. 639–647, May 2007.

[28] Z. Q. Wu, Z. Hao, and D. Yang, "A new MVA sensitivity method for fast accurate contingency evaluation," *Int. J. Electr. Power Energy Syst.*, vol. 38, no. 1, pp. 1–8, Jun. 2012.
[29] K. R. C. Mamandur and G. J. Berg, "Efficient simulation of line and transformer outages in power systems," *IEEE Trans. Power App. Syst.*, vol. PAS-101, no. 10, pp. 3733–3741, Oct. 1982.
[30] A. J. Ardakani and F. Bouffard, "Acceleration of umbrella constraint discovery in generation scheduling problems," *IEEE Trans. Power Syst.*, vol. 30, no. 4, pp. 2100–2109, Jul. 2015.
[31] T. Akbari and M. T. Bina, "A linearized formulation of AC multi-year transmission expansion planning: A mixed-integer linear programming approach," *Electr. Power Syst. Res.*, vol. 114, pp. 93–100, Sep. 2014.
[32] *MATPOWER—A MATLAB Power System Simulation Package v6.0b2*. Accessed: Jun. 30, 2021. [Online]. Available: http://www.pserc.cornell.edu/matpower/

HUANSHENG ZHOU (Member, IEEE) received the B.S. degree in electrical engineering from the Huazhong University of Science and Technology, Wuhan, China, in 2015, and the Ph.D. degree in electrical engineering from the South China University of Technology, Guangzhou, China, in 2020. His research interests include power system optimization and renewable energy and integrated energy systems planning and operation.

KANGLONG YUAN received the B.S. and M.S. degrees from the School of Electric Power Engineering, South China University of Technology, Guangzhou, China, in 2009 and 2013, respectively. His research interest includes power system planning and optimization.

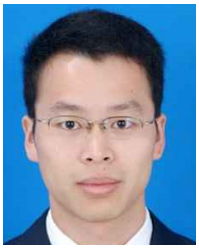

CHENG LEI received the B.S. and M.S. degrees from the College of Electrical Engineering, Sichuan University, Chengdu, China, in 2010 and 2014, respectively. His research interests include power system optimization and renewable energy integration.